Molecular excitation energies to high-lying bound states from time-dependent density-functional response theory: Characterization and correction of the time-dependent local density approximation ionization threshold

Mark E. Casida, Christine Jamorski, Kim C. Casida, and Dennis R. Salahub

Citation: The Journal of Chemical Physics **108**, 4439 (1998); doi: 10.1063/1.475855
View online: http://dx.doi.org/10.1063/1.475855
View Table of Contents: http://scitation.aip.org/content/aip/journal/jcp/108/11?ver=pdfcov
Published by the AIP Publishing

Molecular excitation energies to high-lying bound states from time-dependent density-functional response theory: Characterization and correction of the time-dependent local density approximation ionization threshold

Mark E. Casida,[a] Christine Jamorski,[b] Kim C. Casida, and Dennis R. Salahub
Département de chimie, Université de Montréal, C.P. 6128, Succursale centre-ville, Montréal, Québec H3C 3J7, Canada

(Received 14 November 1997; accepted 11 December 1997)

This paper presents an evaluation of the performance of time-dependent density-functional response theory (TD-DFRT) for the calculation of high-lying bound electronic excitation energies of molecules. TD-DFRT excitation energies are reported for a large number of states for each of four molecules: N_2, CO, CH_2O, and C_2H_4. In contrast to the good results obtained for low-lying states within the time-dependent local density approximation (TDLDA), there is a marked deterioration of the results for high-lying bound states. This is manifested as a collapse of the states above the TDLDA ionization threshold, which is at $-\epsilon_{\mathrm{HOMO}}^{\mathrm{LDA}}$ (the negative of the highest occupied molecular orbital energy in the LDA). The $-\epsilon_{\mathrm{HOMO}}^{\mathrm{LDA}}$ is much lower than the true ionization potential because the LDA exchange-correlation potential has the wrong asymptotic behavior. For this reason, the excitation energies were also calculated using the asymptotically correct potential of van Leeuwen and Baerends (LB94) in the self-consistent field step. This was found to correct the collapse of the high-lying states that was observed with the LDA. Nevertheless, further improvement of the functional is desirable. For low-lying states the asymptotic behavior of the exchange-correlation potential is not critical and the LDA potential does remarkably well. We propose criteria delineating for which states the TDLDA can be expected to be used without serious impact from the incorrect asymptotic behavior of the LDA potential. © *1998 American Institute of Physics.* [S0021-9606(98)01511-6]

I. INTRODUCTION

A quantitative understanding of molecular electronic excited states is important in many domains, including spectroscopy, photochemistry, and the design of optical materials. The prediction or interpretation of the discrete spectrum of many molecules, especially medium size and large molecules, is a demanding task for theoretical methods. Hohenberg–Kohn–Sham density-functional theory[1,2] has been remarkably successful at providing a means of computing a variety of ground state properties to an accuracy which rivals that of considerably more expensive, correlated *ab initio* methods. The important possibility of extending this success to the treatment of molecular excitations is, at present, highly promising. The time-dependent generalization of the density-functional theory formalism offers a rigorous route to the calculation of the dynamic response of the charge density. (For reviews see Refs. 3–7.) Combining this with linear response theory allows the calculation of vertical electronic excitation spectra.[5,8–10]

Initial applications of time-dependent density-functional response theory (TD-DFRT), nearly 20 years ago, to calculate the photoabsorption spectra of atoms[11] (which were based on analogy with time-dependent Hartree–Fock theory and predated the formal development of TD-DFRT) used a scattering theory formulation involving the imaginary part of the complex polarizability, α, and this has remained the standard technique until very recently. In particular, the photoabsorption cross section is proportional to the spectral strength function,

$$S(\omega)=\frac{2\omega}{\pi}\,\mathrm{Im}\,\bar{\alpha}(\omega+i\eta), \tag{1.1}$$

where η is a small positive real number. In the limit $\eta\rightarrow 0$, this becomes a stick spectrum,

$$S(\omega)=\sum_I f_I[\,\delta(\omega-\omega_I)+\delta(\omega+\omega_I)\,], \tag{1.2}$$

while for $\eta\neq 0$ the lines show Lorentzian broadening. This is a natural way to treat the continuum part of the spectrum. Although it can also be used to treat the discrete part of the spectrum, this requires that a nonzero value of η be used (i.e., that the lines be artificially broadened) and spectroscopically dark states cannot be treated at all. Applications have been primarily to calculating photoabsorption cross sections of atoms[11,12] above or near the true ionization threshold, and to modeling (often within sphericalized or jellium models) low resolution photodetachment spectra of metal

[a]e-mail: casida@chimie.umontreal.ca
[b]Present address: l'Institut de Physique Expérimentale, Ecole Polytechnique Fédérale de Lausanne, 1015 Lausanne, Switzerland.

clusters[13–15] and surface excitations.[16] This method has also been tried for molecules (albeit using only single center expansions).[17,18]

Because of the need for an accurate knowledge of the energies of both dipole-allowed and dipole-forbidden transitions, the calculation of the discrete spectrum places much greater demands upon the theoretical method than does production of the spectral function. This is especially true if attention is given to spectroscopic assignments and the ordering of states, rather than just a spectral pattern. Time-dependent density-functional response theory has recently been reformulated to allow the direct calculation of discrete transition energies and oscillator strengths. An early application[19] along these lines was to the jellium-sphere cluster model and made extensive use of spherical symmetry. A formulation suitable for general molecular applications was presented soon thereafter.[5] There is no need for line broadening, and both dark and bright states are obtained in the same manner.

This approach has now been applied to a number of atoms and molecules.[8–10,20,21] In all these studies, the time-dependent local density approximation (TDLDA) has been found to give remarkably good results for transitions to low-lying states. However, a deterioration in the quality of results for higher excitation energies has been noted,[8,20] though results for the higher states were not presented in these studies. The cause of this deterioration was not investigated. Bauernschmitt and Ahlrichs[20] noted that this was also the case for TD-DFRT with other functionals as well as the LDA, and suggested that the problem may lie in the use of the adiabatic approximation, while we[8] suggested that it is due to the onset of the ionization continuum occurring at too low an energy in the TDLDA.

Before the TD-DFRT method can be used reliably for applications, this problem with the ''high-lying'' states needs to be either corrected or clearly delineated, so that the problematic ''high'' states can be recognized even in the absence of any other data against which to compare them. In the present paper, we both propose criteria allowing recognition of the ''high'' states where the TDLDA should not be relied upon, and show that the problem can be largely corrected by using another functional.

It has long been known that the TDLDA ionization threshold is at the negative of the highest occupied molecular orbital (HOMO) energy, $-\epsilon_{\mathrm{HOMO}}^{\mathrm{LDA}}$.[6,11,22] Although minus the HOMO orbital energy should be the exact ionization potential, $I=-\epsilon_{\mathrm{HOMO}}$, in the limit of the exact functional, E_{xc},[23] the LDA HOMO electrons are underbound owing to a too rapid (exponential) asymptotic decay of the LDA exchange-correlation potential, v_{xc}, making the TDLDA ionization threshold substantially too low. Unfortunately, other present popular functionals suffer from the same problem. Although hybrid functionals[24,25] come closer to the correct Coulomb $(-1/r)$ asymptotic behavior of v_{xc}, they go asymptotically as $-a/r$ where a is some constant other than 1.[6] Several authors have reported improved results for the spectral function or selected excitation energies, using various approaches which do give the correct asymptotic behavior. (See Ref. 6 for a brief review.) However, no explicit investigation of the effect of the incorrect location of the TDLDA ionization threshold on TDLDA excitation energies has been undertaken, in spite of the popularity of the TDLDA, e.g., in cluster physics, for calculations of spectra (spectral strength functions) within the jellium sphere and other simplified cluster models.

The dramatic effect of this formal result for practical calculations was shown for the first time by our early results for high-lying discrete transitions of N_2, given in Ref. 6. However, it was also shown that, in the adiabatic approximation, the TD-DFRT ionization threshold lies at $-\epsilon_{\mathrm{HOMO}}^{F}$ for any functional, F.[6] This suggested that the use of an exchange-correlation potential with the correct asymptotic behavior would alleviate the problem of the collapse of the higher excitation energies. In fact, using such a potential in the self-consistent field (SCF) step only (i.e., without coupling the correction) should be sufficient because the TDLDA/F ionization threshold of $-\epsilon_{\mathrm{HOMO}}^{F}$ is already determined at the SCF step. Indeed, our calculations using the 1994 gradient-correction of van Leeuwen and Baerends (LB94),[26] in the SCF step, confirmed this for N_2.[6] Note that the LB94 functional is constructed to have the correct asymptotic behavior, $v_{xc}^{\sigma}(\mathbf{r})\rightarrow -1/r$, for the case of exponentially decaying densities encountered in Coulombic systems.

The present paper gives a more detailed account of this work on N_2, and extends it to three other molecules, namely CO, CH_2O, and C_2H_4, in order to better assess both the effect of the TDLDA ionization threshold on the quality of TDLDA excitation energies, and the extent to which the LB94 functional for the exchange-correlation potential can improve upon the TDLDA. Although the foregoing discussion suggests that TDLDA excitation energies might simply be used as long as they are below $-\epsilon_{\mathrm{HOMO}}^{\mathrm{LDA}}$, as will be seen, this alone is not a sufficient criterion to allow states significantly affected by the incorrect TDLDA threshold to be avoided, and an additional condition will be given.

II. METHOD

Since our methodology has been presented in detail elsewhere,[5,6] only a brief sketch will be given here.

Time-dependent density-functional theory provides a formally rigorous extension of Hohenberg–Kohn–Sham density-functional theory, which is time-independent, to the situation where a system, initially in its ground stationary state, is subject to a time-dependent perturbation modifying its external potential, v.[3,27–35] (Reviews may be found in Refs. 3–7, 16, and 22.) A stationary action principle may be derived, analogous to the minimum energy principle of Hohenberg–Kohn theory, and this can be used, together with appropriate assumptions concerning v-representability, to derive the time-dependent Kohn–Sham equation,

$$\left[-\frac{1}{2}\nabla^2+v(\mathbf{r},t)+\int\frac{\rho(\mathbf{r}',t)}{|\mathbf{r}-\mathbf{r}'|}d\mathbf{r}'+v_{xc}^{\sigma}(\mathbf{r},t)\right]\psi_{j\sigma}(\mathbf{r},t)$$

$$=i\frac{\partial}{\partial t}\psi_{j\sigma}(\mathbf{r},t), \tag{2.1}$$

(in hartree atomic units) where the time-dependent charge density is given by the sum of the orbital densities. Although the v_{xc}^{σ} appearing in the time-dependent Kohn–Sham equation is formally the functional derivative of the exchange-correlation action, $\mathscr{A}_{xc}$, most calculations, including those presented here, make use of the adiabatic approximation,

$$v_{xc}^{\sigma}(\mathbf{r},t)=\frac{\delta \mathscr{A}_{xc}[\rho_{\uparrow},\rho_{\downarrow}]}{\delta\rho_{\sigma}(\mathbf{r},t)}\cong\frac{\delta E_{xc}[\rho_{\uparrow}^{t},\rho_{\downarrow}^{t}]}{\delta\rho_{\sigma}^{t}(\mathbf{r})}, \tag{2.2}$$

where $\rho_{\sigma}^{t}(\mathbf{r})$ is the function $\rho_{\sigma}(\mathbf{r},t)$ evaluated at the fixed time, t. That is, the adiabatic approximation consists of using the same exchange-correlation potential as in the time-independent theory but evaluated using the charge density at time t. In the popular TDLDA, E_{xc} is approximated using the local density approximation (LDA).

Since the dynamic polarizability, $\overline{\alpha}(\omega)$, describes the response of the dipole moment to a time-dependent electric field, it may be calculated from the response of the charge density obtained from time-dependent density-functional theory, hence using time-dependent density-functional response theory (TD-DFRT). This allows the determination of the electronic excitation spectrum in the usual dipole approximation, because according to the sum-over-states relation,

$$\overline{\alpha}(\omega)=\sum_{I}\frac{f_I}{\omega_I^2-\omega^2}, \tag{2.3}$$

the poles of the dynamic polarizability determine the excitation energies, ω_I, while the residues, f_I, determine the corresponding oscillator strengths. (See, e.g., Ref. 5.) A finite basis set formalism is used to cast the dynamic polarizability in the tensorial form of the sum-over-states expression (2.3). Examination of the pole structure then shows that the transition energies may be obtained by solving a matrix eigenvalue problem,

$$\mathbf{\Omega}\vec{F}_I=\omega_I^2\vec{F}_I, \tag{2.4}$$

where $\mathbf{\Omega}$ is defined in Refs. 5, 6, and 8, and the oscillator strengths, f_I, are readily obtained from the eigenvectors, $\vec{F}_I$.

Since TD-DFRT produces transition densities, rather than the N-electron wave functions for the excited states, a complete assignment of term symbols for the transitions obtained typically requires that some additional approximation be introduced. Following Ref. 5, we assume that the wave function, Ψ_I, for the Ith excited state has the form,

$$\Psi_I=\sum_{ij\sigma}^{f_{i\sigma}>f_{j\sigma}}\sqrt{\frac{\epsilon_{j\sigma}-\epsilon_{i\sigma}}{\omega_I}}F_{ij\sigma}^{I}\hat{a}_{j\sigma}^{\dagger}\hat{a}_{i\sigma}\Phi+\cdots, \tag{2.5}$$

where Φ is the single determinant of Kohn–Sham orbitals occupied in the ground state noninteracting system and the creation and annihilation operators, $\hat{a}_{j\sigma}^{\dagger}$ and $\hat{a}_{i\sigma}$, refer to the Kohn–Sham molecular orbital representation. This approximation appears to be quite adequate, and is used in the present work, for the qualitative purpose of assigning term symbols to the quantitative transition energies and oscillator strengths obtained by solving the eigenvalue problem Eq. (2.4).

III. COMPUTATIONAL DETAILS

The TD-DFRT procedure divides naturally into an SCF step and a post-SCF step. We use a notation which reflects the fact that it is possible to use different functionals for the SCF and post-SCF steps. Thus TDLDA/LDA and TDLDA/LB94 indicate that the LDA or LB94 functional, respectively, was used at the SCF step, and TDLDA refers to the functional used to construct the coupling matrix ($\sim \delta v_{\mathrm{SCF}}^{\sigma}/\delta\rho_{\tau}$) in the post-SCF step. In order to make contact with the terminology used elsewhere in the literature, we note that the TDLDA/LDA is often simply referred to as the TDLDA and occasionally as the adiabatic LDA, while the TDLDA/LB94 is simply referred to as LB94, or as the ''model potential'' by Baerends and coworkers.[36–39]

Our TD-DFRT calculations were performed using version 2 of our program deMon-DynaRho (for ''dynamic response of ρ'').[40] This program follows the methodology described in Ref. 5, but differs from version 1[41] (used in Ref. 8) in that it also incorporates improvements along the lines described in Ref. 6. This is a post-SCF program designed to be used with deMon-KS (for ''Kohn–Sham'')[42] for the SCF step. Both of these programs use the same auxiliary basis sets, which improve computational scaling both through the elimination of four-center integrals and by reducing the number of grid points needed to evaluate exchange-correlation terms. Both programs also use the same grid. All calculations were done at the experimental geometries.[43]

Gaussian-type orbital (GTO) basis sets are used for both orbital and auxiliary bases. Our orbital basis was constructed beginning with the medium-sized basis set developed by Sadlej[44,45] for calculating polarizabilities. While the Sadlej basis appears to be flexible enough to describe excitations to valencelike excited states,[8,20,21] we augmented the Sadlej basis set with additional diffuse functions to aid in the description of excitations to Rydberg-like excited states. These exponents were obtained by continuing the observed geometric progression in the Sadlej basis, and are given in Table I. Six Cartesian d-functions were used. This basis set will be referred to as Sadlej+, and consists of 74, 102, and 130 contracted GTOs, for the diatomics, CH_2O, and C_2H_4, respectively. In the case of C_2H_4, one eigenvector of the overlap matrix was eliminated during the SCF step due to an effective linear dependency in the Sadlej+ basis set.

The auxiliary basis sets were chosen from the deMon basis set library: (5,1;5,1) for hydrogen and (4,4;4,4) for C, N, and O. We did not use supplemented auxiliary sets with diffuse functions added, due to convergence difficulties in the SCF step. In tests comparing six different auxiliary basis

TABLE I. Additional diffuse functions added to the Sadlej basis set (Refs. 44 and 45) to make the Sadlej+ basis set.

Atom	Gaussian-type orbital exponents			
	s-exponents		p-exponents	d-exponents
C	0.014 70	0.004 48	0.012 00	0.012 00
N	0.020 20	0.006 08	0.017 30	0.017 30
O	0.027 00	0.008 07	0.019 00	0.019 00
H	0.010 20	0.003 22	0.010 20	none

sets, including supplementation with diffuse functions, the maximum difference in TDLDA/LB94 excitation energies among these auxiliary basis sets was 0.11 eV, for the first six states of formaldehyde. In one test on N_2, (unbalanced) supplementation of the auxiliary basis set resulted in differences of a few tenths of an eV, with the TDLDA/LB94 functional. This level of precision of the TDLDA/LB94 results is adequate for the present work. In contrast, the TDLDA/LDA results do not appear to be significantly affected by the addition of diffuse functions to the auxiliary basis sets used (observed differences being only on the order of a few hundredths of an eV), presumably because of the shorter range of the LDA potential.

The deMon ''extrafine'' ''random'' grid (32 radial and 194 angular points per atom) was used throughout. For CH_2O and C_2H_4, calculations using ''nonrandom'' grids, with C_{2v} and D_{2h} symmetry, respectively, were used to confirm assignments with the LB94 potential because symmetry breaking was observed with the ''random'' grid, in this case, for some of the higher-lying unoccupied orbitals. (Differences between excitation energies with these two grids were insignificant — typically about 0.01 eV or less.)

The SCF calculations were performed with version 1.2 of the deMon-KS module,[42] to which we added the LB94 potential.[26] The SCF convergence criteria were a change of less than 10^{-8} a.u. in the charge density fitting coefficients and, simultaneously, less than 10^{-8} hartree in the total energy. We used the LDA energy expression for both the LDA and the LB94 SCF calculations. In the case of the LB94 potential, this is simply a convenient and harmless choice, which only affects the meaning of the SCF convergence criterion, since only the density (or more exactly the orbitals, orbital energies, and occupations), but not the total energy, enters into the TD-DFRT calculations.

IV. RESULTS AND DISCUSSION

Four small, well-studied molecules, namely N_2, CO, CH_2O, and C_2H_4, have been chosen as test molecules in order to evaluate the quality of the TDLDA/LDA and TDLDA/LB94 excitation energies. These molecules may also be considered as prototypes for studying the (n,π^*) and (π,π^*) transitions important for organic photochemistry. Comparison is made with published single-particle excitation energies from high-quality *ab initio* methods and with experiment. This comparison covers both singlet and triplet states, over a fairly wide range of energies (almost up to the ionization potential.) Theory predicts a number of highly excited states which either do not appear to have been observed experimentally or for which accepted experimental excitation energies are not available. For this reason, our primary comparison is against the *ab initio* calculations. The choice of *ab initio* results against which to compare was governed by the desire to use, insofar as possible, a single set of results for each molecule, that would give reasonably accurate values for all the states considered. The selected calculations are in good agreement with experiment. The state-by-state comparison between the results of different calculations was made by identifying the nth state of a given symmetry from one calculation with the nth state of the same symmetry in the other calculation, with the TD-DFRT N-electron term symbol being determined according to the procedure described in Sec. II. For ethylene, only excitations out of the $1b_{3u}(\pi)$ orbital are considered, and the same state-by-state comparison scheme used for the other molecules is applied to this π-excitation manifold. The results of these comparisons, for the four molecules, are shown in Figs. 1, 2, 3, and 4.

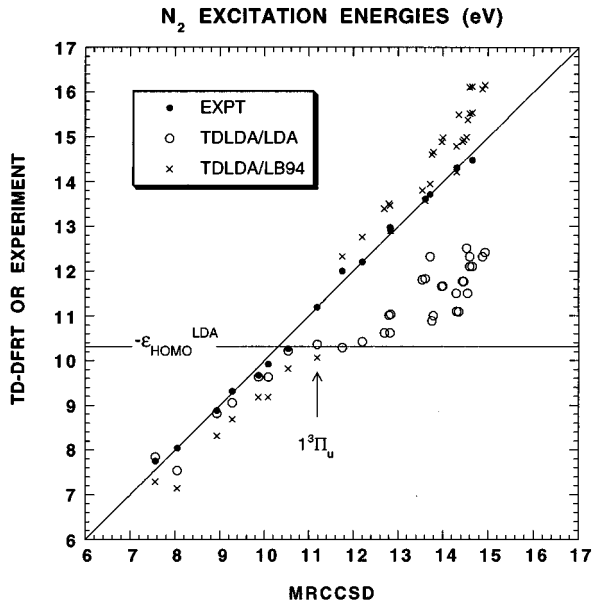

FIG. 1. Correlation plot comparing TD-DFRT results with the multireference coupled cluster singles and doubles (MRCCSD) results of Ref. 53 for the first 35 vertical excitation energies (not counting degeneracies) of N_2. Experimental values taken from Ref. 53 are also shown.

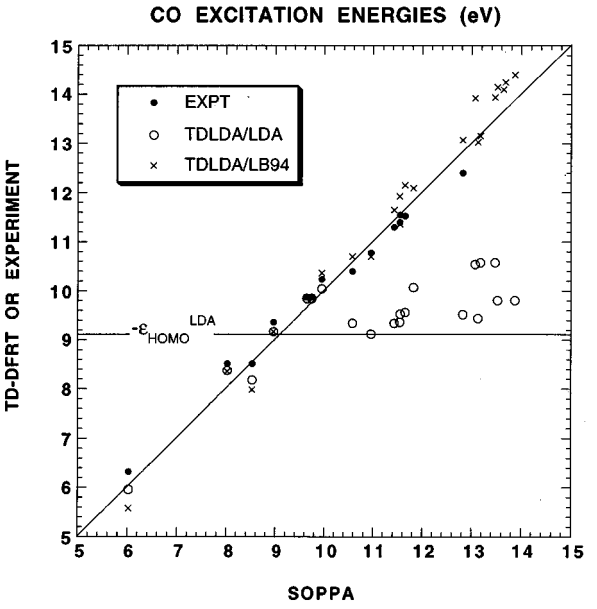

FIG. 2. Correlation plot comparing TD-DFRT results with second-order polarization propagator (SOPPA) ($S\neq 1$ results from Table II of Ref. 54) for the first 23 vertical excitation energies (not counting degeneracies) of CO. Experimental values taken from Ref. 54 are also shown.

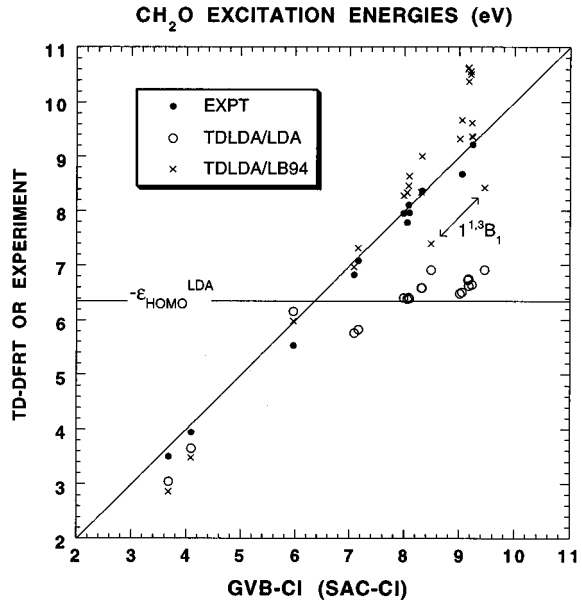

FIG. 3. Correlation plot comparing TD-DFRT results for the first 23 vertical excitation energies (not counting degeneracies) of CH_2O with the generalized-valence-bond configuration-interaction (GVB-CI) results of Ref. 55 ($^{1,3}B_1$ values are symmetry-adapted cluster configuration interaction (SAC-CI) results from Table III of Ref. 56). Experimental values taken from Refs. 57 and 58 are also shown.

A. Effect of the TDLDA ionization threshold

The most striking feature evident from Figs. 1–4 is the collapse of the TDLDA/LDA excitation manifold above $-\epsilon_{\mathrm{HOMO}}^{\mathrm{LDA}}$ in every case, in contrast to the good performance of the TDLDA/LDA below this energy. This is consistent with the formal result that the TDLDA/LDA ionization continuum begins at $-\epsilon_{\mathrm{HOMO}}^{\mathrm{LDA}}$,[6,11,22] which is too low in the LDA compared with the experimental ionization potential (Table II), due to the incorrect asymptotic behavior of the LDA v_{xc}. Thus the collapse occurs because the calculation is attempting to describe a continuum with a finite number of states.

TABLE II. Vertical ionization potentials and $-\epsilon_{\mathrm{HOMO}}$ for the molecules considered in this paper.

Molecule	$-\epsilon_{\mathrm{HOMO}}$ (eV) LDA	$-\epsilon_{\mathrm{HOMO}}$ (eV) LB94	Experimental Ionization Potential (eV)[a]
N_2	10.36	15.90	15.60
CO	9.10	14.32	14.01
CH_2O	6.32	11.78	10.88
C_2H_4	6.91	11.89	10.68

[a]From Refs. 61 (N_2 and CO), 62 (CH_2O), and 63 (C_2H_4).

In this situation it is to be expected that the TDLDA/LDA excitation energies above $-\epsilon_{\mathrm{HOMO}}^{\mathrm{LDA}}$ will be much more sensitive to the diffuseness of the basis set than are the lower states. This is indeed the case, as is illustrated for N_2 in Fig. 5. In fact, the collapse of the higher states is not apparent with the Sadlej basis, though the errors are obviously larger than for the lower states. However, when additional diffuse functions are added to form our Sadlej+ basis, the collapse becomes quite pronounced, as is also the case with the larger JRY118 basis (see caption, Fig. 5). In contrast, the lower states are quite well converged with the Sadlej basis.

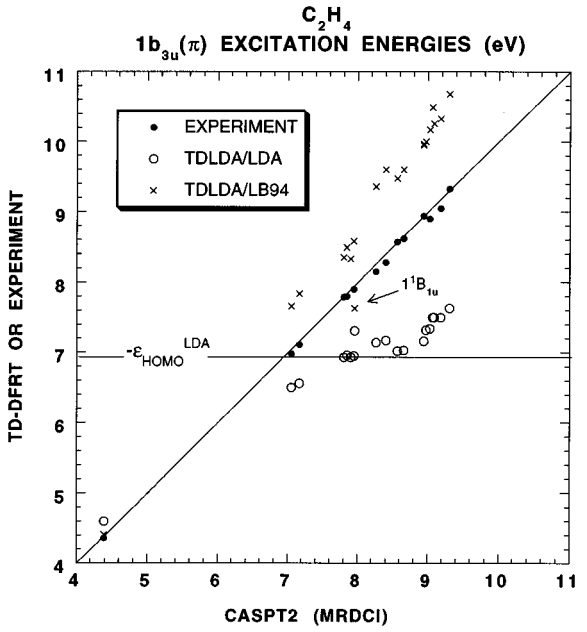

FIG. 4. Correlation plot comparing TD-DFRT results for the first 20 vertical excitation energies (not counting degeneracies) out of the $1b_{3u}(\pi)$ orbital of C_2H_4 with the complete-active-space second-order perturbation theory (CASPT2) results of Ref. 50 ($^1B_{1u}$ value is the more accurate multireference doubles configuration interaction (MRDCI) result of Ref. 59). Experimental values taken from Ref. 50 are also shown.

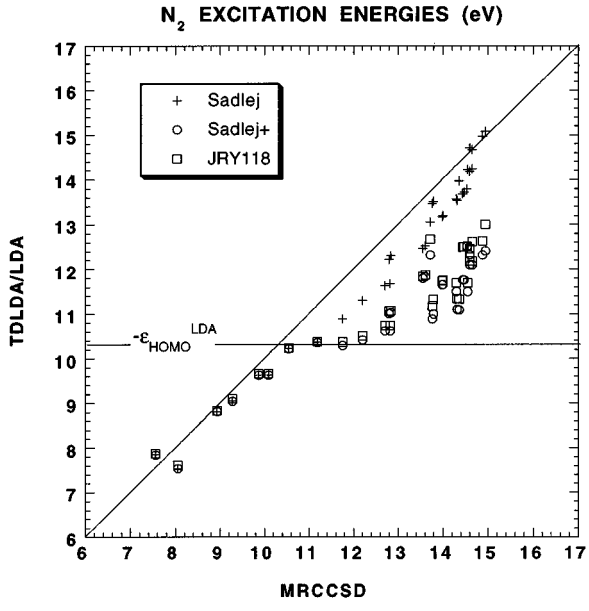

FIG. 5. Effect of the basis set on the N_2 transitions shown in Fig. 1, with the TDLDA/LDA functional. The location of $-\epsilon_{\mathrm{HOMO}}^{\mathrm{LDA}}$ is nearly the same for all three basis sets. The basis sets are Sadlej's 52 contracted Gaussian-type orbital (CGTO) basis set (Refs. 44 and 45), our 74 CGTO Sadlej+ basis set (Table I), and the 118 CGTO JRY118 basis set, identical to the very good basis set of Ref. 60 except that we have neglected the f-functions and retained the s-type component of the 6 Cartesian d-functions.

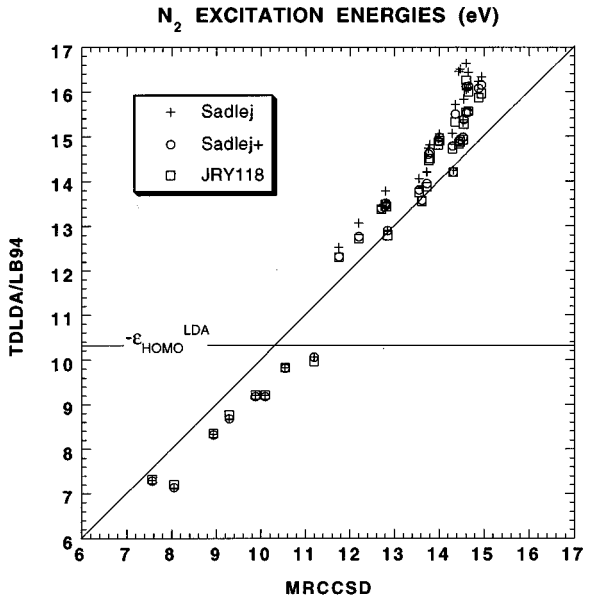

FIG. 6. Effect of the basis set (see caption Fig. 5) on the N_2 transitions shown in Fig. 1, with the TDLDA/LB94 functional.

Since the collapse of the high-lying excitations in the TDLDA/LDA originates from the incorrect asymptotic behavior of the LDA exchange-correlation potential, the use (in the SCF step) of a potential, F, with the correct asymptotic behavior, and hence a value of $-\epsilon_{\mathrm{HOMO}}^{F}$ which more closely approximates the true ionization potential, should rectify the problem. As is seen in Table II, $-\epsilon_{\mathrm{HOMO}}^{\mathrm{LB94}}$ is a much better approximation to the vertical ionization potential than is $-\epsilon_{\mathrm{HOMO}}^{\mathrm{LDA}}$. The TDLDA/LB94 results in Figs. 1–4 show no collapse of the high-lying excitations.

Since the high-lying discrete transitions with the TDLDA/LB94 functional are no longer plagued by artifacts from a finite-basis description of the continuum, they should be much less sensitive to basis set than with the TDLDA/LDA. This is indeed the case, as is seen for N_2 in Fig. 6. Although the higher excitations are, not surprisingly, less well converged with respect to basis set than are the lower states, even the unsupplemented Sadlej basis gives a fair description of the higher states, with transition energies for N_2 which differ from those of the larger Sadlej+ basis by at most about 0.5 eV. The Sadlej+ and JRY118 basis sets yield TDLDA/LB94 transition energies for N_2 which differ by at most 0.2 eV, and typically much less.

B. Closer examination of the TDLDA/LB94 excitation energies

Although the TDLDA/LB94 functional gives a dramatic improvement over the TDLDA/LDA for the high-lying states, it does overestimate the transition energies to most of these states, in some cases by as much as 1 eV or more, though typically much less than this. This is consistent with the observation that the TDLDA/LB94 functional slightly underestimates the mean polarizabilities of these molecules.[36,46] (In the present molecules, almost all the transitions below $-\epsilon_{\mathrm{HOMO}}^{\mathrm{LDA}}$ are dark.) We have found that for mean polarizabilities calculated with the LB94 potential using the finite field method (equivalent to fully coupled LB94,) the LB94 overcorrects the LDA polarizabilities to a considerable extent, yielding a more severe underestimate than with the TDLDA/LB94 functional.[46] So coupling the LB94 gradient correction would be expected to exacerbate rather than alleviate the TDLDA/LB94 overestimate of the high-lying excitation energies.

There are also a few of the higher states for which the TDLDA/LB94 excitation energies are substantially too low (i.e., by 1 eV or more). If we classify the occupied molecular orbitals loosely according to valence-bond concepts as ''π-bonds'' [$1\pi_u$ in N_2, 1π in CO, $1b_1(\pi)$ in CH_2O, and $1b_{3g}(\pi)$ in C_2H_4], ''lone pairs'' [$3\sigma_g$ in N_2, 5σ in CO, and $2b_2(n)$ in CH_2O], and the remaining primarily ''σ-bonds'' (which may or may not contain a lone pair component), then the states with underestimated TDLDA/LB94 excitation energies are excitations out of σ-bonds, although not every excitation out of a σ-bond is underestimated. In particular, the underestimated excitations are the $1\,^3\Pi_u(\mathrm{C})(2\sigma_u,1\pi_g)$ excitation in N_2 and the $1\,^{1,3}B_1[5a_1(n\sigma),2b_1(\pi^*)]$ singlet and triplet excitations in CH_2O (these transitions are indicated in Figs. 1 and 3), and several σ-excitations in C_2H_4.

The π-excitation manifold of ethylene has been extensively studied for spectroscopic, photochemical, and historical reasons, and we have restricted our comparison in Fig. 4 to this manifold. In contrast, much less seems to be known about the σ-excitation manifold. Calculations have been done at the time-dependent Hartree–Fock (TDHF)[47,48] and second-order Møller–Plesset perturbation-theory-corrected configuration-interaction singles (CIS-MP2)[49] levels. These calculations indicate that the first σ-excitations are the $^{1,3}B_{1g}[1b_{3g}(\pi'_{\mathrm{CH}_2}),1b_{2g}(\pi^*)]$ singlet-triplet pair lying at about 8.0–9.5 eV, and an experimental transition at 9.2 eV has been reassigned as the singlet σ-excitation on the basis of TDHF calculations.[47] This is consistent with the expectation that excitations out of the σ-system should occur at significantly higher energies than excitations out of the π-bond. In our TDLDA/LB94 calculation, the $^{1,3}B_{1g}[1b_{3g}(\pi'_{\mathrm{CH}_2}),1b_{2g}(\pi^*)]$ singlet-triplet pair is the second and third excitations at 6.59 (singlet) and 7.08 eV (triplet), which are apparently significantly too low. Other calculations (including TDHF,[47,48] CIS-MP2,[49] second-order polarization propagator (SOPPA),[50] etc.) also find very low-lying $^{1,3}B_{1g}$ states, but they correspond to the $[1b_{3u}(\pi),\ 2b_{2u}(3p_y)]$ orbital promotion. This is clearly different from the TDLDA/LB94 result (differences between Kohn–Sham and Hartree–Fock orbitals notwithstanding) because the $[1b_{3g}(\pi'_{\mathrm{CH}_2}),1b_{2g}(\pi^*)]$ promotion moves charge density *out of* the plane of the molecule, while the $[1b_{3u}(\pi),2b_{2u}(3p_y)]$ moves charge density *into* the plane of the molecule. Other σ-excitations from our TDLDA/LB94 calculations are also much lower in energy than expected.

This makes the separation of the σ- and π-excitation manifolds less clear-cut, since the σ and π excitations may have the same overall symmetry and so couple to each other when they are close in energy. In order to confirm our assignments of π-excitations, we also performed another

TABLE III. N_2 low-lying vertical excitation energies.

	Excitation Energy (eV) Other Theory							Experiment	TDLDA/	
State	MRCCSD	SOPPA	MCTDHF	TDHF	TDHF	CIS	CIS		LDA	LB94
$1\,^3\Sigma_g^+(E)$ $(3\sigma_g,4\sigma_g)$	11.75							12.0	10.29	12.32
$1\,^3\Pi_u(C)$ $(2\sigma_u,1\pi_g)$	11.19	11.05	11.43	11.26	11.28	11.74		11.19	10.36	10.06
TDLDA/LDA Threshold at 10.36 eV										
$1\,^1\Delta_u(w)$ $(1\pi_u,1\pi_g)$	10.54	10.51	10.76	8.75	8.78	9.06	9.09	10.27	10.22	9.82
$1\,^1\Sigma_u^-(a')$ $(1\pi_u,1\pi_g)$	10.09	10.02	10.40	7.94	7.94	8.50	8.51	9.92	9.63	9.18
$1\,^3\Sigma_u^-(B')$ $(1\pi_u,1\pi_g)$	9.87	9.96	10.07	7.94	7.94	8.50	8.51	9.67	9.63	9.18
$1\,^1\Pi_g(a)$ $(3\sigma_g,1\pi_g)$	9.28	9.32	9.60	9.76	9.77	10.02	9.94	9.31	9.05	8.68
$1\,^3\Delta_u(W)$ $(1\pi_u,1\pi_g)$	8.93	8.93	8.86	5.80	5.86	7.33	7.35	8.88	8.82	8.32
$1\,^3\Pi_g(B)$ $(3\sigma_g,1\pi_g)$	8.05	7.87	8.17	7.62	7.62	7.99	7.94	8.04	7.54	7.14
$1\,^3\Sigma_u^+(A)$ $(1\pi_u,1\pi_g)$	7.56	7.91	7.64	3.47	3.46	6.23	6.25	7.75	7.85	7.29
Ground state $1\,^1\Sigma_g^+(\tilde{X})$ at 0.00 eV										
Average error[a]:	0.13	0.15	0.27	1.92	1.91	1.09	1.07		0.19	0.60
Reference	53 Table II	64	60	60	20 Table I	20 Table 1	65 TDA results	53 Table III		

[a]Average absolute deviation from experiment for transitions which meet both of the criteria given in the text.

TDLDA/LB94 calculation with all occupied orbitals except the $1b_{3u}(\pi)$ orbital frozen during the post-SCF step. The energies of most of the excitations out of this orbital differed by less than 0.1 eV between the two calculations, the one notable exception being the ''V transition,'' $1\,^1B_{1u}[1b_{3u}(\pi),1b_{2g}(\pi^*)]$, whose excitation energy is 0.93 eV higher in the frozen orbital calculation. This difference is consistent with the observation that, in a parent molecular orbital description, this excitation is lowered considerably by dynamic correlation involving excitations out of the σ-system (i.e., the σ-system relaxes during this excitation).[51]

Overall, the TDLDA/LB94 gives a reasonable description of most of the high-lying excitations considered in this work. However, further improvement in the functional is clearly desirable.

C. Closer examination of the TDLDA/LDA excitation energies

In contrast to the situation for the high-lying states, it is evident from Figs. 1–4 that the TDLDA/LDA does quite well for excitation energies below $-\epsilon_{\mathrm{HOMO}}^{\mathrm{LDA}}$. However, it is important to be careful about just what is meant by ''states below $-\epsilon_{\mathrm{HOMO}}^{\mathrm{LDA}}$.'' Note that there are a few states where the experimental transition energy is above $-\epsilon_{\mathrm{HOMO}}^{\mathrm{LDA}}$ but the TDLDA/LDA value falls below the TDLDA/LDA ionization threshold of $-\epsilon_{\mathrm{HOMO}}^{\mathrm{LDA}}$. The TDLDA/LDA excitation energies for these states may have substantial errors (e.g., over 1 eV) as is typical of TDLDA/LDA excitation energies above the TDLDA/LDA threshold, and these errors can result in incorrect orderings. This is apparent, for example, for the $1\,^{1,3}B_2[2b_2(n),6a_1(3s)]$ states of formaldehyde, which have fallen below the $1\,^3A_1[1b_1(\pi),2b_1(\pi^*)]$ state, in the TDLDA/LDA. Such ''fallen states'' below $-\epsilon_{\mathrm{HOMO}}^{\mathrm{LDA}}$ are also seen in the TDLDA/LDA results for N_2 and ethylene. (See Tables III–VI.) On the graphs, these TDLDA/LDA excitation energies look like part of the collapse of the higher states, yet they are a little *below* $-\epsilon_{\mathrm{HOMO}}^{\mathrm{LDA}}$.

This too can be understood in terms of the incorrect asymptotic behavior of the exchange-correlation potential which results in the effective potential seen by the LDA or-

TABLE IV. CO low-lying vertical excitation energies.

	Excitation Energy (eV) Other Theory					Experiment	TDLDA/	
State	MRCC	SOPPA	TDHF	TDHF	CIS		LDA	LB94
$1\,^3\Sigma^-(e)$ $(1\pi,2\pi)$	9.82	9.64	9.35	9.38	9.74	9.88	9.84	9.86
$1\,^3\Delta(d)$ $(1\pi,2\pi)$	9.18	8.96	7.90	7.93	8.78	9.36	9.17	9.17
TDLDA/LDA Threshold at 9.10 eV								
$1\,^1\Pi(A)$ $(5\sigma,2\pi)$	8.79	8.53	8.89	8.79	9.07	8.51	8.18	7.98
$1\,^3\Sigma^+(a')$ $(1\pi,2\pi)$	8.26	8.02	6.33	6.36	7.82	8.51	8.37	8.36
$1\,^3\Pi(a)$ $(5\sigma,2\pi)$	6.32	6.02	5.35	5.30	5.88	6.32	5.96	5.58
Ground state $1\,^1\Sigma^+(\tilde{X})$ at 0.00 eV								
Average error[a]:	0.18	0.27	1.18	1.15	0.56		0.28	0.47
Reference	65 Table V DZP basis	54 Table II $S\neq 1$ results	54 Table II RPA results	65 Table V DZP basis	65 Table V TDA, DZP basis	Calc'd in 54 from 43(a)		

[a]Average absolute deviation from experiment for transitions which meet both of the criteria given in the text.

TABLE V. CH_2O low-lying vertical excitation energies.

	Excitation Energy (eV) Other Theory							Experiment	TDLDA/	
State	SAC-CI	MRDCI	CASPT2	GVB-CI	TDHF	CIS	CIS		LDA	LB94
$1\,^1B_2\ [2b_2(n),6a_1(3s)]$	6.99	7.15	7.30	7.16	8.60	8.60	8.623	7.089	5.83	7.32
$1\,^3B_2\ [2b_2(n),6a_1(3s)]$	6.84	7.01		7.08	8.16	8.24	8.297	6.827	5.76	6.97
TDLDA/LDA Threshold at 6.32 eV										
$1\,^3A_1(\tilde{b})\ [1b_1(\pi),2b_1(\pi^*)]$	6.08	6.15	5.99	5.96	1.87	4.85	4.804	5.53	6.16	5.98
$1\,^1A_2(\tilde{A})\ [2b_2(n),2b_1(\pi^*)]$	4.13	4.05	3.91	4.09	4.37	4.55	4.560	3.94	3.65	3.48
$1\,^3A_2(\tilde{a})\ [2b_2(n),2b_1(\pi^*)]$	3.67	3.69	3.48	3.68	3.40	3.72	3.784	3.50	3.04	2.86
Ground state $1\,^1A_1(\tilde{X})$ at 0.00 eV										
Average error[a]:	0.30	0.31	0.17	0.25	1.40	0.50	0.54		0.46	0.52
Reference	56 Table III	singlets 66 triplets 69	67 Table 3	55 Tables IV & V	20 Table 2	20 Table 2	68 Table I 6-31+G*R basis	57,58[b]		

[a]Average absolute deviation from experiment for transitions which meet both of the criteria given in the text.
[b]Electron energy loss spectroscopy (EELS) results from Table 13 of Ref. 57, except $1\,^1B_2$, which is an optical transition energy given in the same table, and $1\,^3B_2$, which is an EELS transition energy from Table 5 of Ref. 58.

bitals being too shallow (typically by several electron volts). The LDA potential would therefore be expected to support too few bound virtual orbitals, and the orbitals close to the top of the potential (very weakly bound) will be too closely spaced compared to the corresponding orbitals in the exact potential which would be further down in the well. Thus the TDLDA/LDA should be expected to give excitation energies that are too low for transitions whose dominant contribution is a promotion to a virtual which is very weakly bound (or unbound) in the LDA.

For each of the four molecules studied here, the LDA potential supports only 2 bound virtuals (with the Sadlej+ basis), whereas the LB94 potential, which has the correct asymptotic behavior, gives 7 – 25 (not counting degeneracies) bound virtuals for these molecules. Except for the core, the energy differences between successive orbitals are quite similar for these two potentials, up through the LUMO (lowest unoccupied molecular orbital). However, in the LDA, the 2nd unoccupied molecular orbital (2UMO) is the highest bound virtual, for these molecules, it is weakly bound, its energy is sensitive to the diffuseness of the basis set suggesting that it samples the long-range part of the potential, and the difference in energy between it and the LUMO is substantially smaller than with the LB94 potential. This is illustrated for N_2 in Table VII. Among the four molecules studied here, there are five transitions [to the $1\,^3\Sigma_g^+(E)(3\sigma_g,4\sigma_g)$ state of N_2, the $1\,^{1,3}B_2[2b_2(n),\ 6a_1(3s)]$ pair of CH_2O, and the $1\,^{1,3}B_{3u}[1b_{3u}(\pi),4a_g(3s)]$ pair of C_2H_4] for which both (i) the primary contribution is an excitation to the 2UMO, and (ii) the TDLDA/LDA excitation energy is below $-\epsilon_{\mathrm{HOMO}}^{\mathrm{LDA}}$. In all five cases, the TDLDA/LDA transition energy is too low (by 0.5 to 1.7 eV). In fact, these are precisely the 5 ''fallen states'' where the experimental transition energy is above the TDLDA/LDA threshold but the TDLDA/LDA excitation energy falls below threshold. Since we have traced this problem to the incorrect asymptotic behavior of the LDA potential, it should be rectified by using the LB94 potential. As is seen in Figs. 1–4, and Tables III–VI, the TDLDA/LB94 functional does indeed fix the problem with these states, though for ethylene it overcorrects. All of the other transitions below $-\epsilon_{\mathrm{HOMO}}^{\mathrm{LDA}}$ consist primarily of excitations to the LUMO and so should not be substantially af-

TABLE VI. C_2H_4 low-lying $1b_{3u}(\pi)$ vertical excitation energies.

	Excitation Energy (eV) Other Theory						Experiment	TDLDA/	
State	SAC-CI	MRDCI	CASPT2	TDHF	CIS	CIS		LDA	LB94
$1\,^1B_{3u}(R)\ [1b_{3u}(\pi),4a_g(3s)]$	7.41	7.13	7.17	7.14	7.15	7.102	7.11	6.56	7.84
$1\,^3B_{3u}(T_R)\ [1b_{3u}(\pi),4a_g(3s)]$	7.24	6.89	7.05	6.88	6.92	6.878	6.98	6.49	7.66
TDLDA/LDA Threshold at 6.91 eV									
$1\,^3B_{1u}(T)\ [1b_{3u}(\pi),1b_{2g}(\pi^*)]$	4.54	4.35	4.39	0.26	3.55	3.543	4.36	4.60	4.41
Ground state $1\,^1A_g(N)$ at 0.00 eV									
Average error[a]	0.18	0.01	0.03	4.10	0.81	0.82		0.24	0.05
Reference	70[b]	71,72[c]	50 Table II PT2F results	20 Table 3	20 Table 3	68 Table V 6-31+G*R basis	50 Table II		

[a]Average absolute deviation from experiment for transitions which meet both of the criteria given in the text.
[b]3,4-excited SAC-CI result in Table III for $1\,^3B_{1u}(T)$. The other transitions are Basis I results from Table VI.
[c]$1\,^3B_{1u}(T)$ and $1\,^1B_{3u}(R)$ are from Table VII of Ref. 71. $1\,^3B_{3u}(T_R)$ is a DZDP basis result from Table 5 of Ref. 72.

TABLE VII. Some orbital energies of N_2, in eV.

Functional	LDA			LB94		
Basis Set	Sadlej	Sadlej+		Sadlej	Sadlej+	
Orbital	ϵ_i	ϵ_i	$\epsilon_i-\epsilon_{i-1}$	ϵ_i	ϵ_i	$\epsilon_i-\epsilon_{i-1}$
$4\sigma_g$ (2UMO)	0.68	−1.28	0.93	−3.17	−3.41	4.73
$1\pi_g$ (LUMO)	−2.21	−2.21	8.15	−8.14	−8.14	7.76
$3\sigma_g$ (HOMO)	−10.36	−10.36	1.48	−15.90	−15.90	1.42
$1\pi_u$	−11.84	−11.84	1.58	−17.33	−17.32	1.74
$2\sigma_u$	−13.41	−13.42	14.93	−19.07	−19.06	14.25
$2\sigma_g$	−28.35	−28.35		−33.30	−33.31	

fected by the too-close spacing of the higher virtuals in the LDA.

The foregoing discussion suggests that the TDLDA/LDA can be used without encountering the serious adverse consequences of the incorrect asymptotic behavior of the LDA exchange-correlation potential, *for states which satisfy both of the following criteria:* (i) The TDLDA/LDA excitation energy is (solidly) less than $-\epsilon_{\mathrm{HOMO}}^{\mathrm{LDA}}$. (ii) The transition does not involve a major contribution from promotions to virtuals which are too close to or above threshold in the LDA potential. Sensitivity of the orbital energy to the basis set may assist in identifying the bound virtuals in question.

For the present molecules, the second criterion restricts use of the TDLDA/LDA to transitions which consist primarily of a promotion to the LUMO. However, the number of unoccupied orbitals which meet criterion (ii) will depend on the chemical species. For example, the LDA effective potential for Li_4 supports a much larger number of bound virtuals, so more of these will meet criterion (ii) than is the case for the molecules in the present study. An examination of the TDLDA/LDA functional for the discrete spectrum of alkali metal clusters will be the subject of a future paper.

Tables III–VI compare the results of our TD-DFRT calculations with those from *ab initio* methods and with experiment, for the four molecules studied in this paper. Average absolute deviations from experiment are given for all states whose TDLDA/LDA transitions satisfy the two criteria given above. TDHF is the method which is most closely related to TD-DFRT. However, TDHF has the largest average error (1.75 eV for the specified states in all four molecules). Such a large average error is associated with the well-known problem of ''near triplet instabilities'' in the TDHF method. When only the singlets are included in the average, the average error reduces to 0.93 eV. This is very similar to the average error of the CIS method, which is 0.86 eV (for all four molecules). While the CIS method bears many similarities to the TDHF method, it is not a response theory method and thereby avoids the problem of near triplet instabilities. In contrast to TDHF and CIS, the average error (over the four tables) for the high-quality *ab initio* methods (MRCCSD, SOPPA, MCTDHF, CASPT2, GVB-CI, etc.) is 0.20 eV, but these methods involve significantly more costly calculations. In comparison, the TDLDA/LDA does quite well for transitions satisfying the two key criteria, with an average error (0.27 eV over the four molecules) approaching that of the high-quality *ab initio* methods. Yet the computational effort involved is comparable to that for TDHF or CIS. This is all the more noteworthy in view of the similarity of the TD-DFRT and TDHF formalisms. Bauernschmitt and Ahlrichs[20,52] have examined the instability conditions in TD-DFRT and argued that the triplet instability should be less likely to be encountered in TD-DFRT than in TDHF. (See also the discussion in Refs. 5 and 8 about the relative simplicity of the DFT response equations compared with HF.) The average error (for these same states) for the TDLDA/LB94 functional is 0.52 eV. Unlike the TDLDA/LDA, the TDLDA/LB94 results are sensitive to the choice of auxiliary basis set (see Sec. III), so the magnitude of these relatively small differences in average error may change as the auxiliary basis is improved. Nevertheless, the TDLDA/LB94 does seem to do better than CIS, but not quite as well as the TDLDA/LDA, for these low-lying transitions.

V. CONCLUSION

We have presented TD-DFRT results for the bound transitions of four small molecules, including high-lying bound states. Our work confirms the previous observation[8,20] that the TDLDA/LDA gives remarkably good results for low excitation energies. However the quality deteriorates for higher excitation energies. This is to be expected[8] based upon the formal result[6,11,22] that the TDLDA/LDA ionization threshold lies at $-\epsilon_{\mathrm{HOMO}}^{\mathrm{LDA}}$, which is significantly lower than the true ionization potential due to the well-known incorrect asymptotic behavior of the LDA exchange-correlation potential. The present work (as well as the early results presented in Ref. 6) provides the first concrete illustration of the substantial impact of the location of the TDLDA/LDA ionization threshold on the calculation of higher excitation energies. This is particularly important since there is no explicit description of the continuum in the finite basis set methods commonly applied to calculate the discrete spectra of molecules, and the ''collapse of the continuum'' may go entirely unnoticed if an insufficient basis set is used. We have shown that the early onset of the TDLDA/LDA ionization continuum may be corrected by using the LB94 functional in the SCF step. This functional provides an exchange-correlation potential with the correct $(-1/r)$ asymptotic behavior and $-\epsilon_{\mathrm{HOMO}}^{\mathrm{LB94}}$ is much closer to the true ionization potential than is the case for the LDA.

While the TDLDA/LB94 functional gives a dramatic improvement for higher excitation energies, some problems remain. Most of these excitation energies are overestimated. Furthermore, certain ones of the excitations out of the σ-system are underestimated. In both cases, errors can be substantial (i.e., 1 eV or more), though most transition energies are better than this. The TDLDA/LB94 functional gives a reasonably good description of excitations out of the n and π orbitals, which are the primary source of oscillator strength in these molecules. In particular, the (n,π^*) and (π,π^*) excitations, important for organic photochemistry, are reasonably well described. (Note that the nature of the problematic σ-system excitations does not suggest a problem with purely σ-bonded molecules. Further investigation is needed for that case.)

For low-lying excitation energies, the TDLDA/LDA does remarkably well. In fact, for these states, it appears to do better than the TDLDA/LB94 functional, and would be the preferred functional for practical applications where only low-lying excited states are needed. For this reason, it is important to have an *a priori* scheme for identifying those states which may be significantly affected by the incorrect asymptotic behavior of the LDA exchange-correlation potential. Clearly this means restricting attention to excitations below $-\epsilon_{\mathrm{HOMO}}^{\mathrm{LDA}}$. However, we have shown that a second criterion is also necessary, namely the avoidance of excitations to orbitals lying too close to the threshold region of the LDA effective potential. These criteria should also apply to the commonly used gradient-corrected functionals. For states satisfying these two criteria, performance of the TDLDA/LDA is quite good, with an average absolute error much closer to that of the more costly correlated *ab initio* methods than to those for TDHF or CIS. Further studies should be done to determine whether these excellent results of the TDLDA/LDA persist for a variety of molecules.

As in time-independent DFT, the domain of applicability of TD-DFRT ultimately rests on the development and validation of suitable practical functionals. Our results confirm the promise of TD-DFRT for discrete molecular spectra, and indicate where and how the TDLDA/LDA can be improved for molecular applications. A further improvement will be the subject of a subsequent paper.

ACKNOWLEDGMENTS

M.E.C. thanks Dr. Michel R. J. Hachey for an interesting discussion of the excited states of formaldehyde. Financial support through grants from the Natural Sciences and Engineering Research Council (NSERC) of Canada and the Fonds pour la formation des chercheurs et l'aide à la recherche (FCAR) of Québec is gratefully acknowledged.

[1] P. Hohenberg and W. Kohn, Phys. Rev. B **136**, 864 (1964).
[2] W. Kohn and L. J. Sham, Phys. Rev. A **140**, 1133 (1965).
[3] E. K. U. Gross and W. Kohn, Adv. Quantum Chem. **21**, 255 (1990).
[4] E. K. U. Gross, C. A. Ullrich, and U. J. Gossmann, in *Density Functional Theory*, edited by E. K. U. Gross and R. M. Dreizler, NATO ASI Series (Plenum, New York, 1994), p. 149.
[5] M. E. Casida, in *Recent Advances in Density Functional Methods, Part I*, edited by D. P. Chong (Singapore, World Scientific, 1995), p. 155.
[6] M. E. Casida, in *Recent Developments and Applications of Modern Density Functional Theory*, edited by J. M. Seminario, *Theoretical and Computational Chemistry Vol. 4* (Elsevier Science, Amsterdam, 1996), p. 391.
[7] E. K. U. Gross, J. F. Dobson, and M. Petersilka, in *Density Functional Theory II*, edited by R. F. Nalewajski, *Vol. 181 of Topics in Current Chemistry* (Springer, Berlin, 1996), p. 81.
[8] C. Jamorski, M. E. Casida, and D. R. Salahub, J. Chem. Phys. **104**, 5134 (1996).
[9] M. Petersilka, U. J. Gossmann, and E. K. U. Gross, Phys. Rev. Lett. **76**, 1212 (1996).
[10] M. Petersilka and E. K. U. Gross, Int. J. Quant. Chem. Symp. **30**, 181 (1996).
[11] A. Zangwill and P. Soven, Phys. Rev. A **21**, 156 (1980).
[12] K. Nuroh, M. J. Stott, and E. Zaremba, Phys. Rev. Lett. **49**, 862 (1982).
[13] G. Bertsch, Comput. Phys. Commun. **60**, 247 (1990).
[14] M. Brack, Rev. Mod. Phys. **65**, 677 (1993).
[15] A. Rubio, J. A. Alonso, X. Blase, L. C. Balbás, and S. G. Louie, Phys. Rev. Lett. **77**, 247 (1996).
[16] A. Liebsch, *Electronic Excitations at Metal Surfaces* (Plenum, New York, 1997).
[17] Z. H. Levine and P. Soven, Phys. Rev. Lett. **50**, 2074 (1983).
[18] Z. H. Levine and P. Soven, Phys. Rev. A **29**, 625 (1984).
[19] C. Yannouleas, E. Vigezzi, and R. A. Broglia, Phys. Rev. B **47**, 9849 (1993).
[20] R. Bauernschmitt and R. Ahlrichs, Chem. Phys. Lett. **256**, 454 (1996).
[21] R. Bauernschmitt, M. Häser, O. Treutler, and R. Ahlrichs, Chem. Phys. Lett. **294**, 573 (1997).
[22] G. D. Mahan and K. R. Subbaswamy, *Local Density Theory of Polarizability* (Plenum, New York, 1990).
[23] C. O. Almbladh and U. von Barth, Phys. Rev. B **31**, 3231 (1985).
[24] A. D. Becke, J. Chem. Phys. **98**, 1372 (1993).
[25] A. D. Becke, J. Chem. Phys. **98**, 5648 (1993).
[26] R. van Leeuwen and E. J. Baerends, Phys. Rev. A **49**, 2421 (1994).
[27] E. Runge and E. K. U. Gross, Phys. Rev. Lett. **52**, 997 (1984).
[28] A. K. Dhara and S. K. Ghosh, Phys. Rev. A **35**, 442 (1987).
[29] D. Mearns and W. Kohn, Phys. Rev. A **35**, 4796 (1987).
[30] V. Peuckert, J. Phys. C **11**, 4945 (1978).
[31] S. Chakravarty, M. B. Fogel, and W. Kohn, Phys. Rev. Lett. **43**, 775 (1979).
[32] B. H. Deb and S. K. Ghosh, J. Chem. Phys. **77**, 342 (1982).
[33] L. J. Bartolotti, Phys. Rev. A **24**, 1661 (1981).
[34] L. J. Bartolotti, Phys. Rev. A **26**, 2243 (1982).
[35] H. Kohl and R. M. Dreizler, Phys. Rev. Lett. **56**, 1993 (1986).
[36] S. J. A. van Gisbergen, V. P. Osinga, O. V. Gritsenko, R. van Leeuwen, J. G. Snijders, and E. J. Baerends, J. Chem. Phys. **105**, 3142 (1996).
[37] S. J. A. van Gisbergen, J. G. Snijders, and E. J. Baerends, Chem. Phys. Lett. **259**, 599 (1996).
[38] S. J. A. Gisbergen, J. G. Snijders, and E. J. Baerends, Phys. Rev. Lett. **78**, 3097 (1997).
[39] V. P. Osinga, S. J. A. van Gisbergen, J. G. Snijders, and E. J. Baerends, J. Chem. Phys. **106**, 5091 (1997).
[40] deMon-DynaRho version 2, M. E. Casida, C. Jamorski, and D. R. Salahub, University of Montreal.
[41] deMon-DynaRho version 1, C. Jamorski, M. E. Casida, and D. R. Salahub, University of Montreal.
[42] (a) A. St-Amant and D. R. Salahub, Chem. Phys. Lett. **169**, 387 (1990); (b) Alain St-Amant, Ph.D. Thesis, Université de Montréal (1992); (c) deMon-KS version 1.2, J. W. Andzelm, M. E. Casida, A. Koester, E. Proynov, A. St-Amant, D. R. Salahub, H. Duarte, N. Godbout, J. Guan, C. Jamorski, M. Leboeuf, V. Malkin, O. Malkina, F. Sim, and A. Vela, deMon Software, University of Montreal, 1995.
[43] Taken from (a) K. P. Huber and G. Herzberg, *Molecular Spectra and Molecular Structure. IV. Constants of Diatomic Molecules* (van Nostrand Reinhold, New York, 1979), for N_2 (p. 420) and CO (p. 166); (b) J. H. Callomon, E. Hirota, K. Kuchitsu, W. J. Lafferty, A. G. Maki, and C. S. Pote, *Landolt-Börnstein, Numerical Data and Functional Relationships in Science and Technology: Vol. 7. Structure of Free Polyatomic Molecules*, edited by K.-H. Hellwege and A. M. Hellwege (Springer-Verlag, New York, 1976), for C_2H_4 (r_0, θ_0) (p. 179) and CH_2O (p. 132).
[44] A. J. Sadlej, Collect. Czech. Chem. Commun. **53**, 1995 (1988).
[45] A. Sadlej, Theor. Chim. Acta **79**, 123 (1991).
[46] M. Castro, M. E. Casida, K. C. Casida, C. Jamorski, and D. R. Salahub (unpublished).
[47] T. D. Bouman and A. E. Hansen, Chem. Phys. Lett. **117**, 461 (1985).
[48] V. Galasso, J. Mol. Struct.: THEOCHEM **168**, 161 (1988).
[49] K. B. Wiberg, C. M. Hadad, J. B. Foresman, and W. A. Chupka, J. Phys. Chem. **96**, 10,756 (1992).
[50] L. Serrano-Andrés, M. Merchán, I. Nebot-Gil, R. Lindh, and B. O. Roos, J. Chem. Phys. **98**, 3151 (1993).
[51] W. T. Borden and E. R. Davidson, Acc. Chem. Res. **29**, 67 (1996).
[52] R. Bauernschmitt and R. Ahlrichs, J. Chem. Phys. **104**, 9047 (1996).
[53] U. Kaldor and S. B. Ben-Shlomo, J. Chem. Phys. **92**, 3680 (1990).
[54] E. S. Nielsen, P. Jørgensen, and J. Oddershede, J. Chem. Phys. **73**, 6238 (1980).
[55] L. B. Harding and W. A. Goddard III, J. Am. Chem. Soc. **99**, 677 (1977).
[56] H. Nakatsuji, K. Ohta, and K. Hirao, J. Chem. Phys. **75**, 2952 (1981).
[57] D. J. Clouthier and D. A. Ramsay, Annu. Rev. Phys. Chem. **34**, 31 (1983).
[58] S. Taylor, D. G. Wilden, and J. Comer, Chem. Phys. **70**, 291 (1982).
[59] C. Petrongolo, R. J. Buenker, and S. D. Peyerimhoff, J. Chem. Phys. **76**, 3655 (1982).
[60] M. Jaszuński, A. Rizzo, and D. L. Yeager, Chem. Phys. **136**, 385 (1989).
[61] D. W. Turner, C. Baker, A. D. Baker, and C. R. Brundle, *Molecular Photoelectron Spectroscopy* (Wiley, New York, 1970).

[62] C. R. Brundle, M. B. Robin, N. A. Kuebler, and H. Basch, J. Am. Chem. Soc. **94**, 1451 (1972).
[63] G. Bieri and L. Åsbrink, J. Electron Spectrosc. Relat. Phenom. **20**, 149 (1980).
[64] J. Oddershede, N. E. Grüner, and G. H. F. Diercksen, Chem. Phys. **97**, 303 (1985).
[65] S. Pal, M. Rittby, R. J. Bartlett, D. Sinha, and D. Mukherjee, J. Chem. Phys. **88**, 4357 (1988).
[66] M. R. J. Hachey, P. J. Bruna, and F. Grein, J. Phys. Chem. **99**, 8050 (1995).
[67] M. Merchaan and B. O. Roos, Theor. Chim. Acta **92**, 227 (1995).
[68] J. B. Foresman, M. Head-Gordon, J. A. Pople, and M. J. Frisch, J. Phys. Chem. **96**, 135 (1992).
[69] P. J. Bruna, M. R. J. Hachey, and F. Grein, J. Phys. Chem. **99**, 16576 (1995).
[70] H. Nakatsuji, J. Chem. Phys. **80**, 3703 (1984).
[71] R. J. Buenker, S. D. Peyerimhoff, and S.-K. Shih, Chem. Phys. Lett. **69**, 7 (1980).
[72] R. B. Buenker and S. D. Peyerimhoff, Chem. Phys. **9**, 75 (1976).